# Calculation of Spur Gear Tooth Flexibility by the Complex Potential Method

A. Cardou
G. V. Tordion
Dept. of Mechanical Engineering, Laval University
Quebec, P.Q., Canada G1K7P4

## Introduction

Calculation of gear tooth flexibility is of interest for at least two reasons: (a) It controls, at least in part, the vibratory properties of a transmission system hence, fatigue resistance and noise; (b) it controls load sharing in multiple tooth contact.

Earlier works on that subject are by Walker[1,2] and by Weber,[3] from the experimental and analytical point of view, respectively. More recently, the finite element method has been used,[7,9] as well as a modified beam theory.[10]

The Complex Potential Method (CPM), based on the conformal mapping of a tooth profile onto the half plane, is another interesting approach in that it provides analytical expressions for stresses and displacements. The accuracy of the results thus obtained depends only on the accuracy of the conformal transformation. Details on the CPM method can be found elsewhere.[6,11]

Calculation of tooth flexibility by the Complex Potential Method has already been presented by Premilhat et al.[8] However, two difficulties were pointed out in that paper, which do not occur in stress calculations: (a) the indeterminacy of the displacements; (b) the singularity at the point of interest, that is the teeth contact point. The first problem was not addressed in reference,[8] while the second was circumvented by calculating deflections on the tooth axis instead of at the contact point, thus losing the effect of local compression. The present paper is an attempt to show how these two problems can be dealt with in order to obtain a more accurate value of tooth flexibility at each point of the line of action for a given pair of spur gears. Detailed calculations can be found in reference.[13]

## Basic Displacement Equations

It has been shown[11] that, for one tooth protruding out of a half plane, and subjected to a concentrated normal force $W$ (Fig. 1), displacements $u$ and $v$ are given by:

$$2\mu(u+iv) = \kappa\phi(\zeta) - \frac{\omega(\zeta)}{\bar{\omega}'(\bar{\zeta})}\,\overline{\phi'(\zeta)} - \overline{\psi(\zeta)} \tag{1}$$

where $\omega(\zeta)$ is the conformal mapping of the tooth profile:

$$z = \omega(\zeta) = c\zeta + \sum_{k=1}^{n} \frac{a_k}{\zeta - ib_k} \tag{2}$$

and the potentials $\phi(\zeta)$ and $\psi(\zeta)$ are given by:

$$\phi(\zeta) = -\frac{W}{2\pi} e^{i\beta}\log(\zeta-\zeta_o) - \sum_{k=1}^{n} \frac{a_k}{\zeta - ib_k} \cdot \frac{\bar{\phi}'(ib_k)}{\bar{\omega}'(ib_k)} \tag{3}$$

$$\psi(\zeta) = \frac{W}{2\pi} e^{-i\beta}\log(\zeta-\zeta_o) - \frac{\bar{\omega}(\zeta)}{\omega'(\zeta)}\,\phi'(\zeta) + \sum_{k=1}^{n} \frac{a_k}{\zeta + ib_k}\,\frac{\phi(-ib_k)}{\omega'(-ib_k)} \tag{4}$$

Coordinates $(x, y)$ in the $z$-plane are in inches, that is, they correspond to a diametral pitch $P = 1$. For any other pitch, one should multiply them by $1/P$. The same remark applies to the various figures of this paper.

Parameters $c$, $a_k$, $b_k$ ($k = 1, 2, \ldots, n$) have to be calculated for each given profile. Once they are known, one sees that displacements $u$ and $v$ can be obtained from equation

**Table 1 Conformal mapping parameters: standard AGMA profile (20 teeth, 20 deg)**

| $k$ | $a_k$ | $b_{(3)}$ |
|---|---|---|
| 1 | 0.249242305 | 0.435215176 |
| 2 | 0.101283187 | 0.099594373 |
| 3 | 0.011811730 | 0.020010559 |
| 4 | 0.001711074 | 0.004242494 |
| | $c = 0.946769291$ | |

---

**AUTHORS:**

**MR. ALAIN CARDOU** *is a professor of mechanical engineering at Laval University, Quebec City, Canada. Dr. Cardou received his BS from Ecole Nationale Supérieure de Mécanique, France, and his MS and PhD from the University of Minnesota, in the area of Mechanics and Materials. He is conducting research on the stress and strength analysis of various mechanical elements. He is a member of ASME.*

**MR. GEORGES V. TORDION** *is a professor of mechanical engineering at Laval University, Quebec City, Canada. After receiving his engineering degree from the Swiss Federal Institute of Technology in Zurich, he worked for the Escher-Wyss Co., Zurich. He became a mechanical engineering professor at the Zurich State College of Engineering in Winterthur and, later, at Laval University. His main research interest has always been in gear technology: kinematics, dynamics, strength, production, lubrication. He is a member of ASME and academic member of AGMA. In 1983, he received the AGMA "Edward P. Connell" Award in recognition of his contribution to the advanced gear research and engineering education. He is a member of IFToMM (International Federation for the Theory of Machines and Mechanisms), and the French language editor of the Journal of Machines and Mechanisms.*

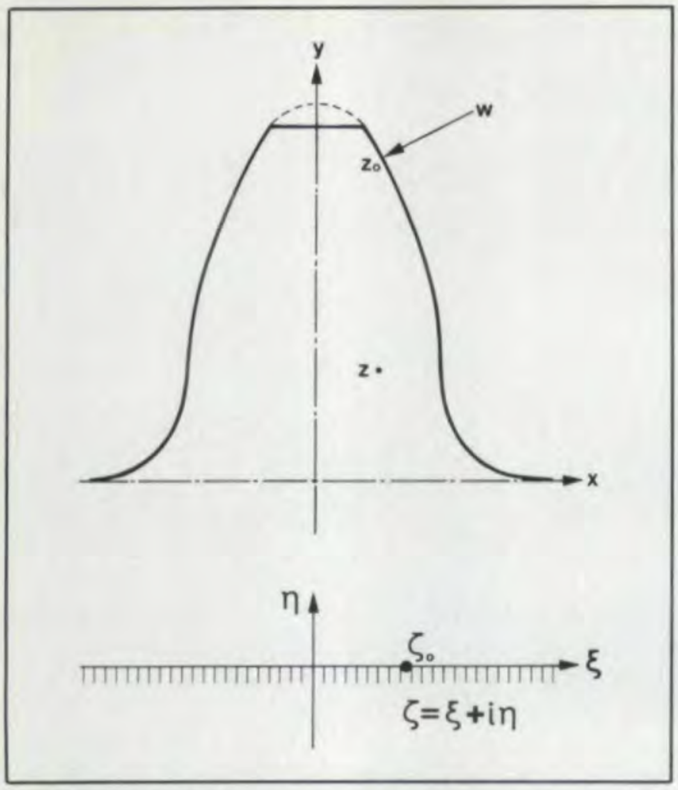


Fig. 1—Conformal mapping of a spur gear tooth.

(1). As an example, transformation parameters for a standard AGMA profile (20 teeth, 20 deg pressure angle) are given in Table 1. Explicit formulas yielding $u$ and $v$ in terms of these parameters have already been reported by Cardou and Tordion[11] and are much too cumbersome to be repeated here.

However, potentials $\phi(\zeta)$ and $w(\zeta)$, and thus $u$ and $v$, are defined within an arbitrary constant. Besides, the elastic domain being semi-infinite, they are unbounded as $z$ (or $\zeta$) tends to infinity. However, for large enough $z$, $\phi$ and $\psi$ are equivalent to their log $(\zeta - \zeta_o)$ term, showing that $u$ and $v$ increase very slowly. Finally $u$ and $v$ are singular for $\zeta = \zeta_o$, that is near the loading point.

### Indeterminacy of Displacements

Although a minor problem from the mathematical point of view, indeterminacy of displacements cannot be treated lightly for practical applications. Indeed, a shift in the displacements yields a corresponding increase or decrease of the tooth flexibility. If one compares the displacements or flexibility curves published by various authors, (see, for example reference),[9] one notices that, although very similar in shape, they appear shifted from one another; the shifts are so large that one can get values differing by more than 100 percent for a given tooth.

The way to eliminate the arbitrary constants is to select a reference point and subtract its displacements from those obtained at the point of interest with the same formulae. Alternatively, an equivalent approach is to define a point as fixed in the solid. The disagreement between published displacement curves seems to come mainly from the selection of a reference point (or of a fixed boundary).

It is shown in Fig. 2 how nondimensional displacements **u** and **v** vary along the axis of a standard tooth under tip loading. For example, if one takes the reference point on the axis, at $3.4/P$ from the pitch circle, the displacement **u** at the tip is 15.3. At $5.4/P$ it is 15.6, and at $7.5/P$ it is 15.7, a variation of less than 1 percent. Thus, it is important to select the reference point deep enough. However, beyond a certain depth, displacements vary very slowly. For thin rim gears, the reference point should of course, be chosen within the rim (and rim deformation should be taken into account separately).

In the following study, the reference point is taken on the tooth axis at twice the tooth height under the root circle. For a standard AGMA profile, this corresponds to a depth of $4.5/P$ from the root circle or $5.75/P$ from the pitch circle.

### Displacements at the Contact Point

In order to obtain the flexibility of a given pair of mating teeth, one has to obtain the displacement component of the contact point in the direction of the line of action. However, as mentioned earlier, equations (1) to (4) have been obtained for a concentrated load $W$, which makes these equations singular precisely at the contact point. Three approaches may be considered to avoid that problem:

(a) Calculate the displacements on the line of action at a given depth under the surface. This approach has been used in reference,[8] where the selected point is the in-

Fig. 2—Tooth axis displacements for tip loading (Standard AGMA profile, 20 teeth, 20 deg).

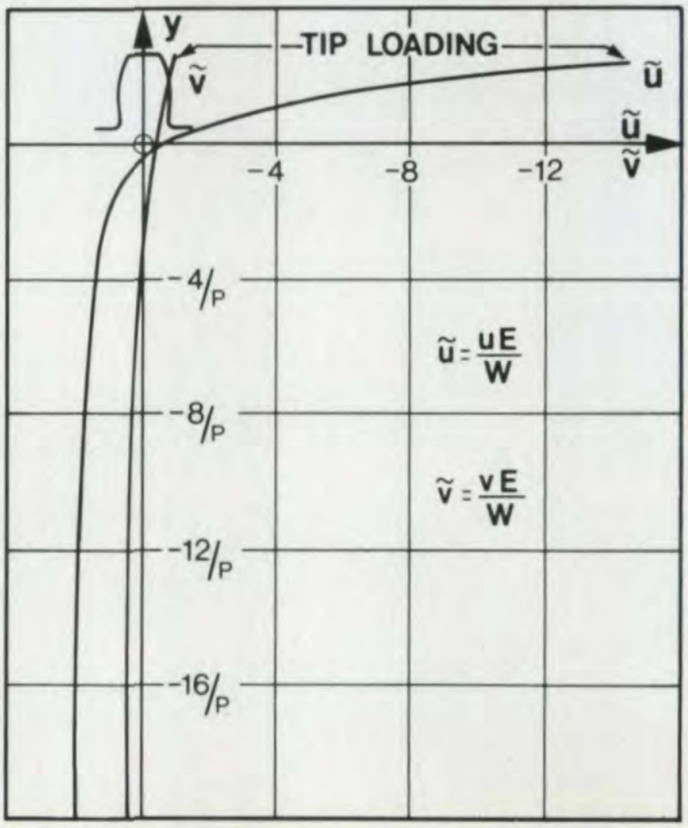

tersection between tooth axis and line of action. By doing so, one loses the local pressure displacements.

(b) Instead of a concentrated load, take a distributed one and recalculate the potentials. This is, of course, the mathematically exact approach. However, it leads to very cumbersome calculations only to get a correct displacement field near the load. Moreover, these expressions depend in a nonlinear fashion on the pair of mating gears, and on the load transmitted.

(c) Utilize the point load solution and correct it near the point of contact. In this approach, one considers that in the immediate neighborhood of that point, displacements behave in the same fashion as for a half plane under the same type of load, either concentrated or distributed. It is indeed possible, in this case, to establish a relationship between the two types of solution and apply it to the tooth problem. This is shown in the following.

Displacements for points on the line of action, calculated with the point load solution are shown in Fig. 3, for three locations of the contact point. It appears that the shape of the curves for points near the surface are almost identical, thus showing that the displacement gradient at those points is independent of the shape of the solids in contact. This leads us to the half-plane problem.

### The Half-Plane Solutions

Nondimensional displacement $\mathbf{v}_{P_o}$ on the axis of a normal load $W$ acting on a half plane is given, within a constant, by:

$$\mathbf{v}_{P_o} = \mathbf{v}_P(0,y) = \frac{2(1-\nu^2)}{\pi}\log|y| - \frac{1+\nu}{2\pi} \tag{5}$$

Now, consider an elliptic pressure $p$ (Fig. 4):

$$p = \frac{2W}{\pi b^2}\sqrt{b^2-x^2} \tag{6}$$

such that
$$W = \frac{\pi b\, p_{\max}}{2} \tag{7}$$

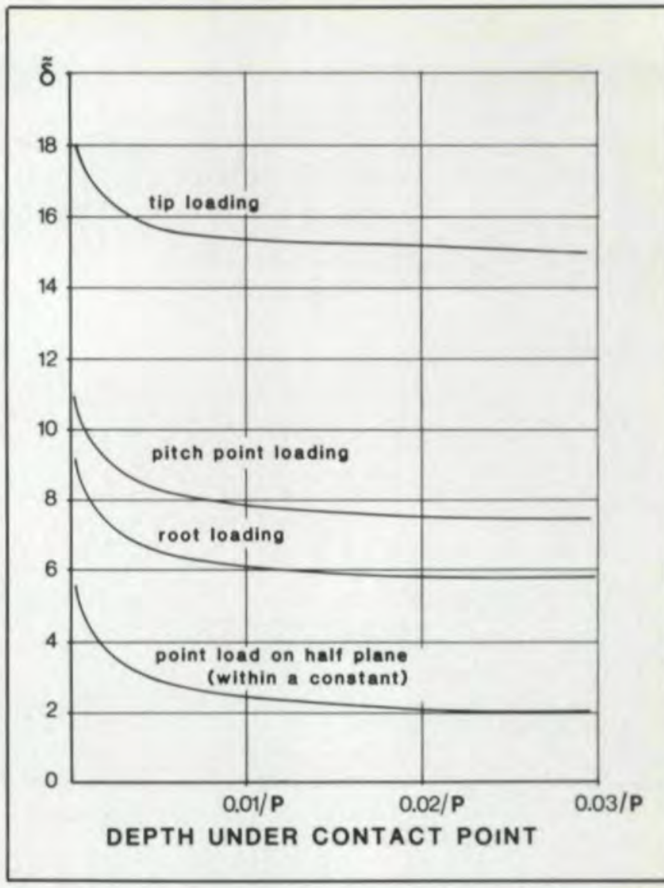


Fig. 3 – Displacement $\bar{\delta}$ of points located on the line of action versus depth under the surface; point load at tip, pitch point, and root of tooth; comparison with corresponding half-plane solution.

Using Westergaard's potentials,[5] one finds the corresponding displacement of a Hertz elliptical distribution load, within a constant, as:

$$\mathbf{v}_{H_o} = -\frac{2(1-\nu^2)}{\pi}\log\left[\frac{y}{b}+\sqrt{1+\left(\frac{y}{b}\right)^2}\right] + \frac{2\nu(1+\nu)}{\pi}\,\frac{y}{b}\left[\sqrt{1+\left(\frac{y}{b}\right)^2}+\frac{y}{b}\right]+C \tag{8}$$

### Nomenclature

$a_k$, $b_k$, $c$ = conformal mapping parameters
$b$ = width of contact zone
$C$ = arbitrary constant
$E$ = Young's modulus
$h$ = depth under the contact point for equivalent displacement calculation
$i$ = imaginary constant $i = \sqrt{-1}$
$p$ = contact pressure
$P$ = diametral pitch
$u,v$ = displacements in $x$, $y$ directions, respectively
$v_H$ = displacement corresponding to an elliptically distributed load (Hertz' theory)
$v_P$ = displacement corresponding to a point load
$v_{H_o}$, $v_{P_o}$ = displacements along $y$-axis at $x = 0$
$W$ = normal load/width
$x,y$ = z-plane coordinates (diametral pitch $P = 1$)
$z$ = defines the location of any material point in the plane $z = x + iy$
$z_o$ = location of contact point in the z-plane
$\beta$ = angle between $x$-axis and line of action ($W$)
$\delta$ = displacement of points of the line of action in its direction
$\delta_o$ = displacement of contact point
$\zeta$ = location of a material point in the conformally transformed plane $\zeta = \xi + i\eta$
$k$ = material constant $k = 3 - 4v$
$v$ = Poisson's ratio
$\mu$ = Lamés parameter $\mu = E/2\,(1 + v)$
$\mu,\xi$ = $\zeta$-plane coordinates
$\varphi,\psi$ = complex potentials
$\omega$ = conformal mapping function, $z = \omega(\zeta)$
$\bar{z},\bar{y},\bar{\varphi},\bar{\psi}$ = complex conjugates of corresponding functions
$\mathbf{v},\bar{\delta}$ = nondimensional displacements $v = uE/W$ $\delta = \delta E/W$

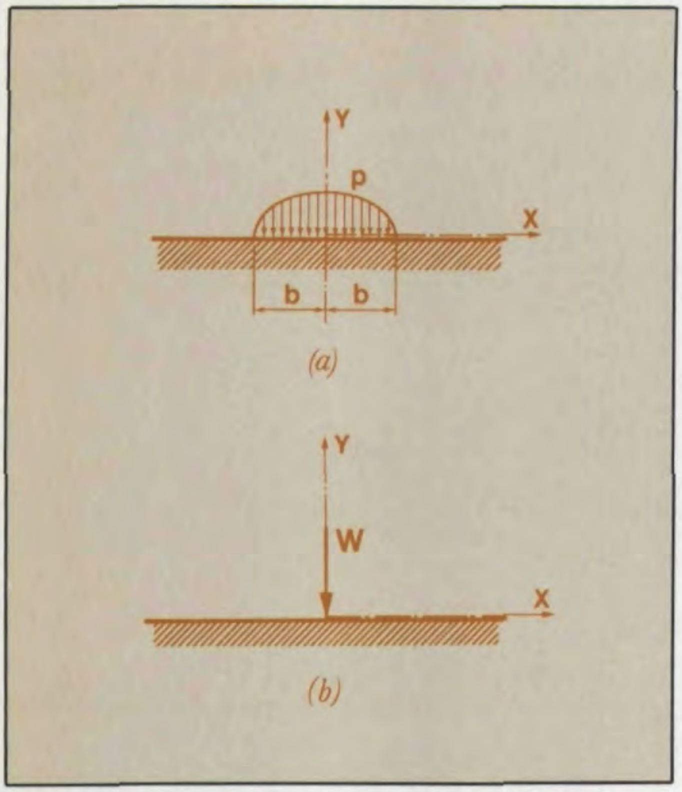


Fig. 4 – Half-plane cases: (a) elliptically distributed load (b) point load.

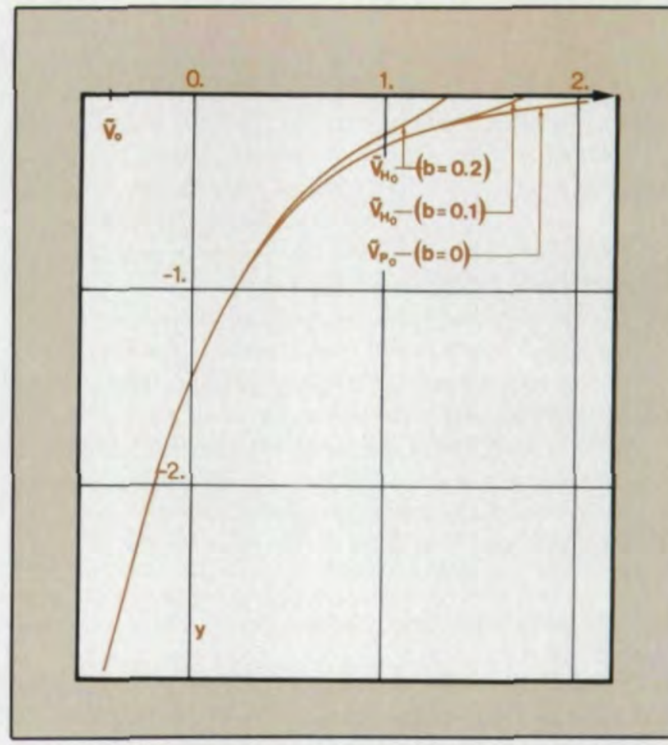


Fig. 5 – Half-plane solutions: comparison of displacements $\bar{v}_{H_o}$ ($b$ = 0.1, 0.2) and $\bar{v}_{P_o}$ ($b$ = 0).

Obviously, far enough from the boundary, solution (8) should converge to solution (5). Thus, letting $y$ tend to $-\infty$ in equation (8) and comparing with equation (5) yields the constant $C$:

$$C = \frac{1+\nu}{\pi}\left[2(1-\nu)\log\frac{b}{2} + \nu - \frac{1}{2}\right] \tag{9}$$

Thus, in the case of the elliptic load, displacement at the boundary point $x = y = 0$ is obtained from equations (8) and (9):

$$\mathbf{v}_{H_o}(0) = C = \frac{1+\nu}{\pi}\left[2(1-\nu)\log\frac{b}{2} + \nu - \frac{1}{2}\right] \tag{10}$$

Typical curves $\mathbf{v}_{P_o}$ and $\mathbf{v}_{H_o}$ are represented in Fig. 5. One sees that, at certain depth $y_o$ under the surface (Fig. 6):

$$\mathbf{v}_{H_o}(0) = \mathbf{v}_{P_o}(y_o) \tag{11}$$

Letting $h = |y_o|$, this relation yields:

$$h = \frac{b}{2}\, e^{\nu/2(1-\nu)} \tag{12}$$

a simple linear relationship between $h$ and $b$. For example for $v$ = 0.3:

$$h = 0.6195\, b \tag{13}$$

Thus, considering that, in the immediate neighborhood of the contact point, relative displacement solutions are practically identical for the tooth and half-plane problems, equation (12) allows one to use the point-load solution to calculate displacements at a distance $h$ below the surface, on the line of action. These displacements are then equal to those arising from an elliptically distributed load. Parameter $b$ has to

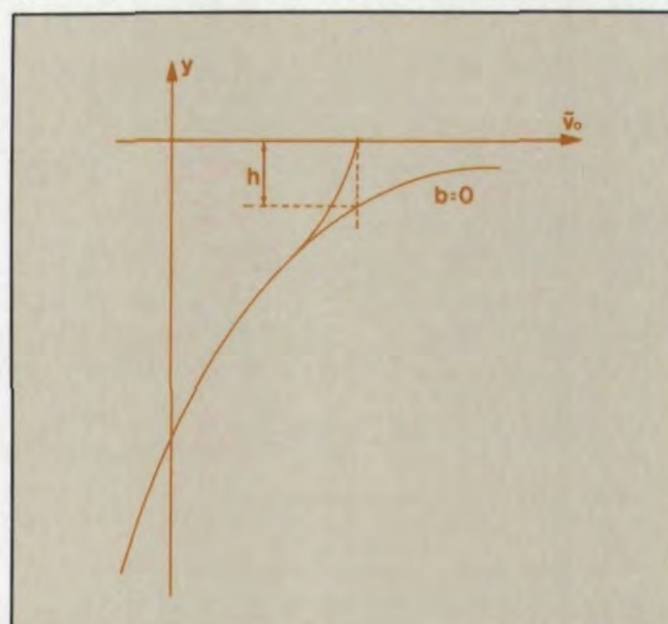


Fig. 6 – Equivalent depth $h$ for surface displacement calculation.

be calculated using the classical Hertz formulas[14] and will depend on the mating gears (size and material), on the load transmitted, and on the location on the line of action, since profile curvature varies from point to point.

### Calculation of Tooth Flexibility

Fig. 7 shows nondimensional displacement curves $\delta_o$ calculated for a standard AGMA profile (30 teeth, 20 deg) as a function of the contact point abscissa on the line of action and for depths $h$ = 0.0015 in., 0.01 in., 0.1 in. under

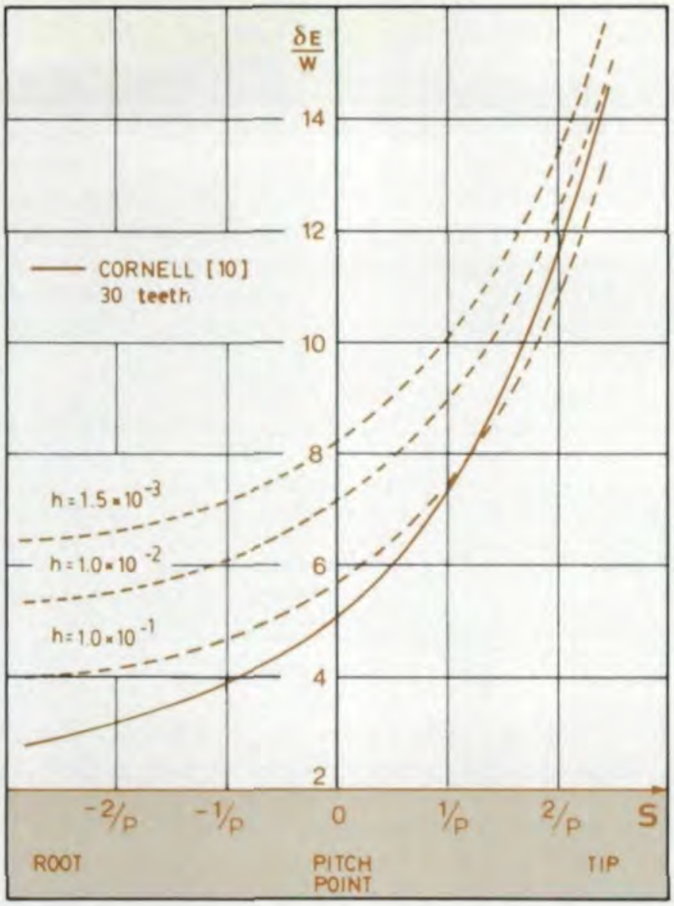


**Fig. 7** – Displacement $\bar{\delta}_0$ versus abscissa of load on line of action; standard AGMA gear (30 teeth, 20 deg); calculation depths: $h$ = 0.0015 in., 0.01 in., 0.1 in. under contact point

the surface. It is important to note that these curves are independent of the absolute dimensions of the gear. The flexibility curve obtained by Cornell[10] for the same profile is also shown in Fig. 7. It does not include the local deformation since that deformation would depend on the mating gears geometry, as well as on materials and transmitted loads.

Indeed, for a given pair of gears, and a given tangential load $W$, one has to calculate the corresponding depth of calculation $h$ at each loading point. The resulting flexibility curve is shown in Fig. 8 for the particular case of a pair of identical standard AGMA gears with the following characteristics:

| | |
|---|---|
| number of teeth: | 20 |
| pressure angle: | 20 deg |
| pitch $P$: | 1 |
| material: | steel |
| pressure at pitch point: | 200 MPa |

Besides, if the contact ratio is taken into account, there is a decrease in the load $W$ when two pairs are in contact. Paradoxically, the flexibility curves seems to indicate a slightly higher nominal deflection in that case than when only one pair is in contact. This is due to the fact that, for a given pressure at pitch point, contact pressure is lower in the double contact region, yielding a smaller contact width $b$, and a smaller depth $h$. Thus, nondimensional flexibility curves $\boldsymbol{\delta}_o = \delta E/W$ are discontinuous between single and double contact regions, owing to the fact that contact pressure is nonlinearly related to $W$.

In the load-sharing case, one should calculate deflections iteratively since pairs of gears, at a given instant, have a different flexibility. Thus to know how they share the total load $W$, one has to know the flexibility curve.

That effect on nondimensional displacement $\boldsymbol{\delta}_o = \delta_o E/W$ is due mainly to the Hertz effect (local compression), which varies as $W^{1/2}$, and it is easily verified that very little discrepancy is obtained on the nondimensional flexibility curve by letting each pair in contact share the load equally. The approximate curve thus obtained can then be used to calculate the real distribution.

Finally, the global flexibility curve for a given pair of gears is obtained by adding the separate curves for each gear. Fig. 9 shows the case of a pair of identical standard AGMA gears with indicated parameters. The CPM flexibility curve is compared with that obtained using Weber's approach. In this case, agreement is quite good except for a shift of one curve with with respect to the other, due to a different way of selecting a reference point.

## Conclusion

It has been shown how expressions obtained through CPM, in the point load case, can be used to calculate displacements at the contact point of a given pair of spur gears. First, a proper reference point has to be selected; then, displacements have to be calculated at a certain depth under the surface. That depth has been shown to vary linearly with the width

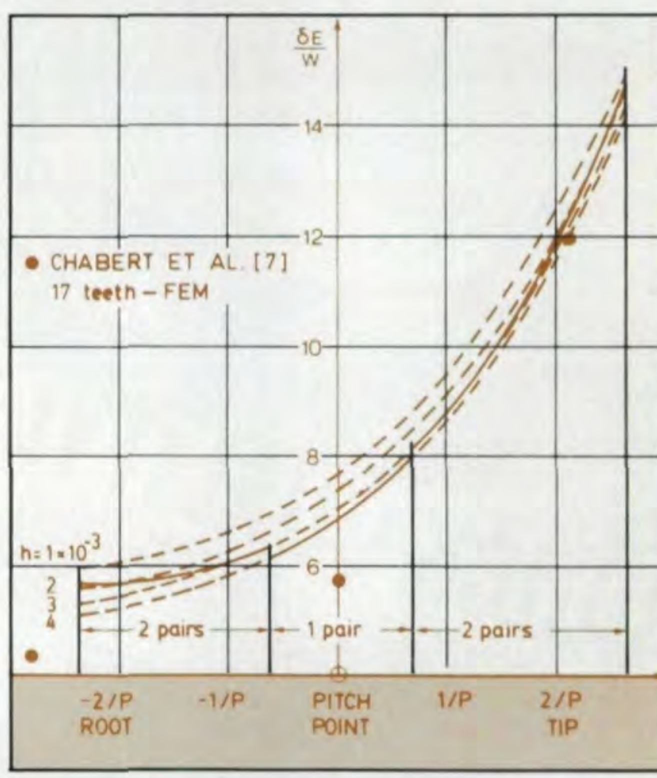


**Fig. 8** – Displacement $\bar{\delta}_0$ versus abscissa of load on line of action for a standard AGMA gear (20 teeth, 20 deg) meshing with an identical gear; maximum pressure at pitch point: 200 MPa, $P$ = 1.

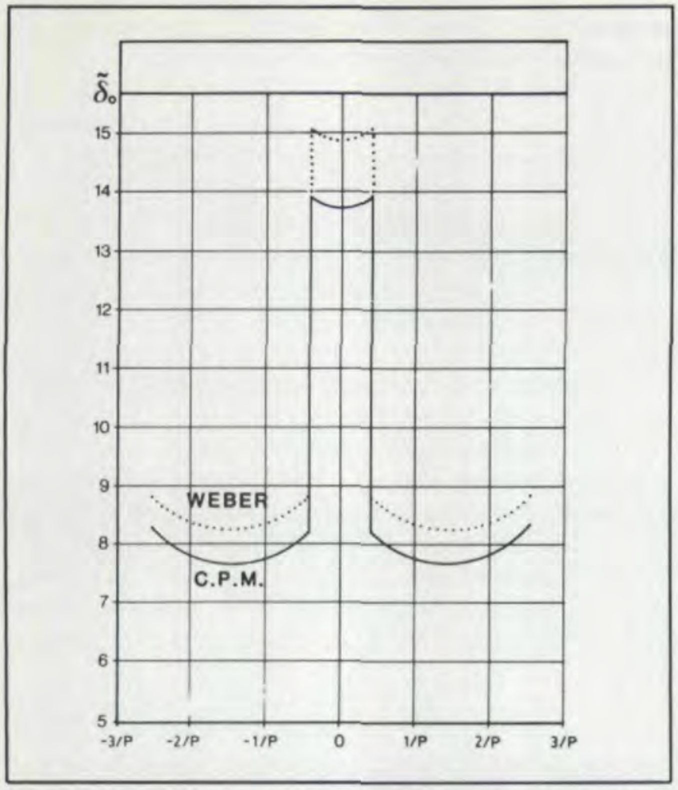


Fig. 9 – Combined flexibility curve $\tilde{\delta}_0$ versus abscissa of load on line of action for a pair of identical standard AGMA gears (40 teeth, 20 deg); $W$ = 1 000 lb/in., $P$ = 0.5, comparison with Weber's curve.



of the contact zone as calculated from Hertz's theory. Contact width may be calculated at each point on the line of action and depends in a nonlinear fashion on absolute dimensions, material properties and transmitted load. This being known, the flexibility curve for the given pair of gears may be obtained, including the load sharing effect. Comparison with published results by Weber,[3] Chabert,[7] and Cornell[10] shows good agreement regarding the shape of flexibility curves, except for a slight shift between these curves, which is due, probably, to the selection of different reference points.


**Acknowledgement:** *Financial support from the National Sciences and Engineering Research Council of Canada is gratefully acknowledged. The authors wish also to thank Mr. A. Fortin for his help in numerical applications.*

*This paper was presented at the Design Engineering Technical Conference, Cambridge, Mass., 1984 of the American Society of Mechanical Engineers. Paper No. 84-DET-85.*


**References**


1. WALKER, M., "Gear Tooth Deflection and Profile Modifications: No. 1," *The Engineer*, Oct. 14, 1938, pp. 409-412.
2. WALKER, M., "Gear Tooth Deflection and Profile Modification: No. 2," *The Engineer*, Oct. 21, 1938, pp. 434-436.
3. WEBER, C., "The Deformation of Loaded Gears and the Effect on their Load-Carrying Capacity; Part I: Elastic Deformation of the Teeth and the Adjoining Parts of the Body of the Wheel," *Dept. of Scientific and Indus. Res.*, Sponsored Research (Germany), Report No. 3, (N. Report No. 102), 1949.
4. RICHARDSON, H. H., "Static and Dynamic Load, Stress and Deflection Cycles In Spur Gear Systems," *Ph.D. thesis*, M.I.T., Cambridge, MA, 1958.
5. WESTERGAARD, H.M., "Bearing Pressures and Cracks," ASME *Journal of Applied Mechanics*, Vol. 6, June 1939, pp. 49-53.
6. BARONET, C. N., and TORDION, G. V., "Exact Stress Distribution in Standard Gear Teeth and Geometry Factors," ASME *Journal of Engineering for Industry*, Vol. 95, No. 4, Nov. 1973, pp. 1159-1163.
7. CHABERT, G., DANG TRAN, T., and MATHIS, R., "An Evaluation of Stresses and Deflections of Spur Gear Teeth Under Strain," ASME *Journal of Engineering for Industry*, Vol. 96, No. 1, Feb. 1974, pp. 85-93.
8. PREMILHAT, A., TORDION, G. V., and BARONET, C. N., "An Improved Determination of the Elastic Compliance of a Spur Gear Tooth Acted on by a Concentrated Load," ASME *Journal of Engineering for Industry*, Vol. 96, No. 2, May 1974, pp. 382-384.
9. TOBE, T., KATO, M., INOUE, K., "True Stress and Stiffness of Spur Gear Tooth," *Proc. of the Fifth World Cong. on Th. of Mach. and Mech.*, Paris, 1979, pp. 1105-1108.
10. CORNELL, R. W., "Compliance and Stress Sensitivity of Spur Gear Teeth," ASME *Journal of Mechanical Design*, Vol. 103, No. 2, Apr. 1981, pp. 447-459.
11. CARDOU, A., and TORDION, G. V., "Numerical Implementation of Complex Potentials for Gear Tooth Stress Analysis," ASME *Journal of Mechanical Design*, Vol. 103, No. 2, Apr. 1981, pp. 460-465.


*(continued on page 46)*

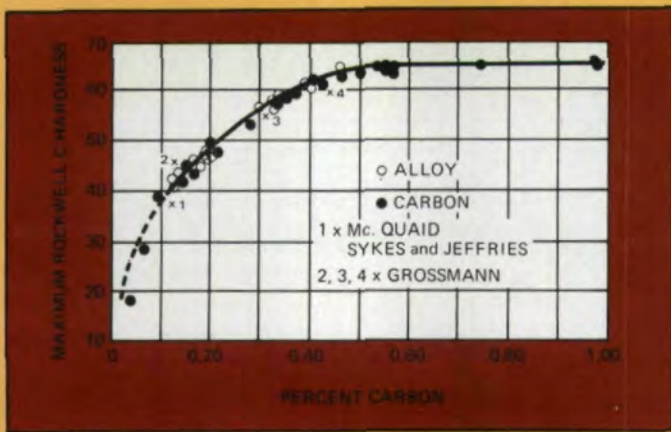


Fig. 1 – Relationship of maximum quenched hardness of alloy and carbon steels to carbon content. *Courtesy Republic Steel Corp.*

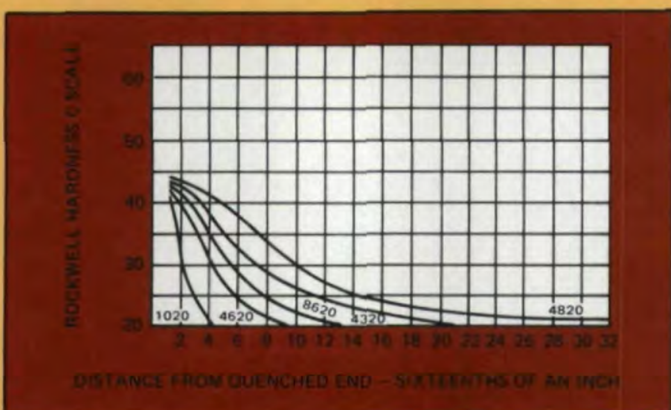


Fig. 2 – Comparative hardenability of 0.20-percent carbon alloy steels. *Courtesy Republic Steel Corp.*

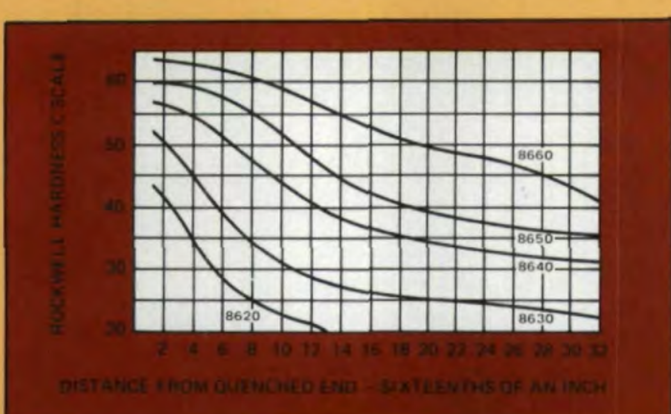


Fig. 3 – Comparative hardenability of 8600 Alloy Steels. *Courtesy Republic Steel Corp.*

on carbon content, Fig. 1. Also, section thickness has considerable influence on the maximum hardness obtained for a given set of conditions; the thicker the section, the slower the quench rate will be. Variations in test bar hardenability curves for various 0.20-percent carbon and alloy steels is shown in Fig. 2. Similar hardenability curves for 8600 alloy steels with various carbon contents is shown in Fig. 3. Maximum hardenability of case-hardened 8620 steel is achieved, Fig. 4, when the case carbon concentration is 0.80-percent.

H-steels are guaranteed by the supplier to meet established hardenability limits for specific grades of steel. These steels

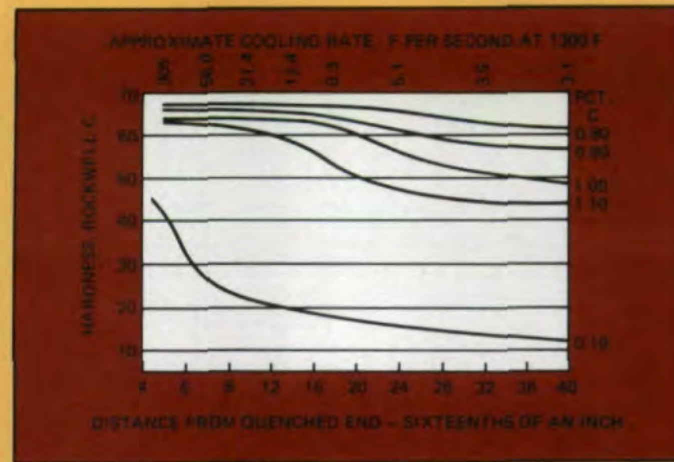


Fig. 4 – Curves showing that maximum hardenability of 8620 steel is achieved when case carbon concentration is at 0.80-percent carbon. *Courtesy Climax Molybdenum Co.*

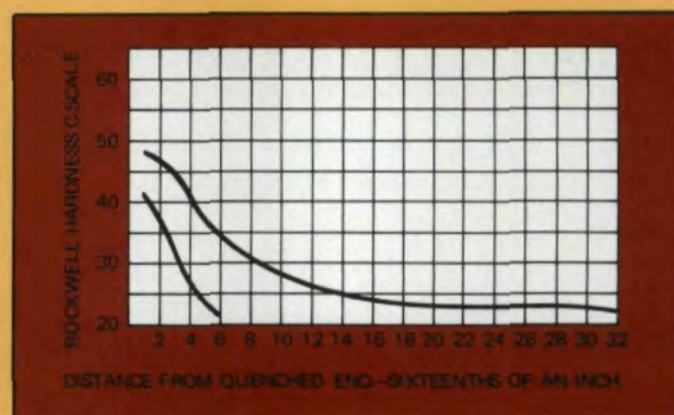


Fig. 5 – Hardenability upper and lower curve limits for 8620H steel. *SAE Iron and Steel Handbook Supplement 30.*

are designated by an "H" following the composition code number, such as 8620H, Fig. 5. Hardenability of H-steels and a steel with the same chemical composition is not necessarily the same. Therefore, H-steels are often specified when it is essential that a given hardness be obtained at a given point below the surface of a gear tooth.

**E-5 ON READER REPLY CARD**

**Acknowledgement:** *Reprinted from Modern Methods of Gear Manufacture, 4th Edition, published National Broach and Machine Division of Lear Siegler, Inc., 17500 Twenty Three Mile Rd., Mt. Clemens, MI 48044.*

## CALCULATION OF SPUR GEAR TOOTH . . .

*(continued from page 14)*

12. TERAUCHI, Y., and NAGAMURA, K., "Study on Deflection of Spur Gear Teeth," *Bull. of JSME,* Vol. 24, No. 188, Feb. 1981, pp. 447-452.
13. FORTIN, A., "Application de la méthode des potentiels complexes aux calculs des déplacements dans les engrenages droits," M.Sc. thesis, Laval University, Quebec, Canada, June 1983.
14. TIMOSHENKO, S. P., and GOODIER, J. N., *Theory of Elasticity,* McGraw-Hill, New York, 3rd ed., 1970.

**E-1 ON READER REPLY CARD**